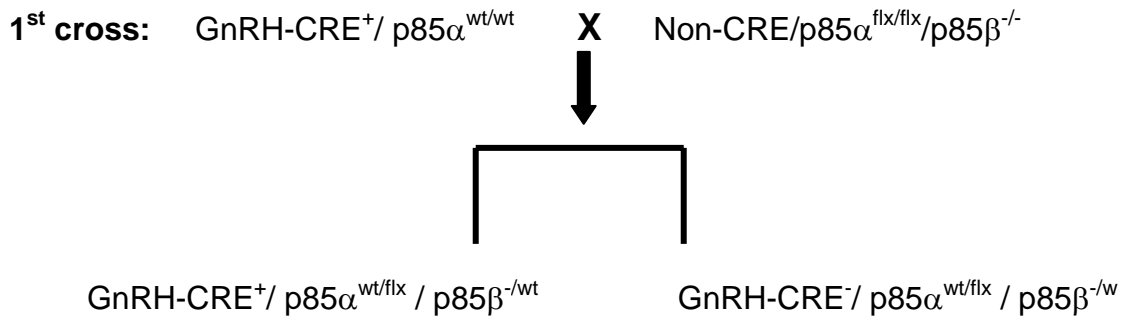
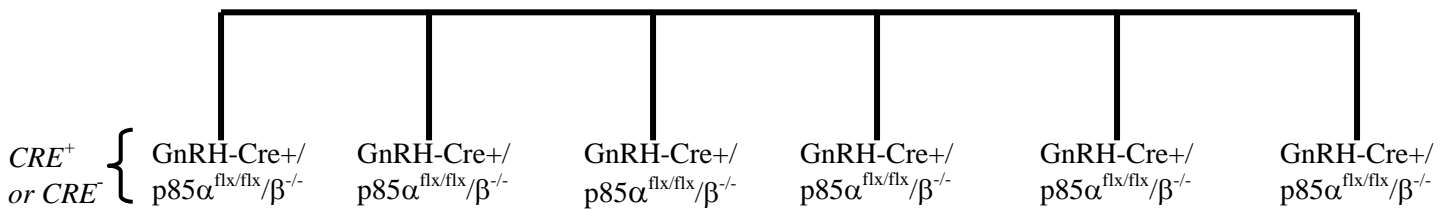
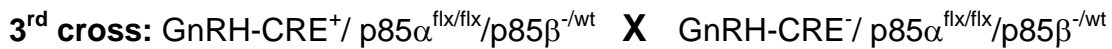
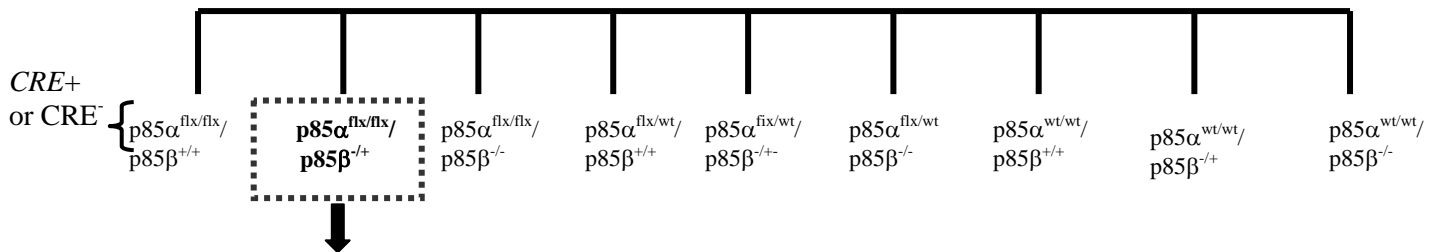


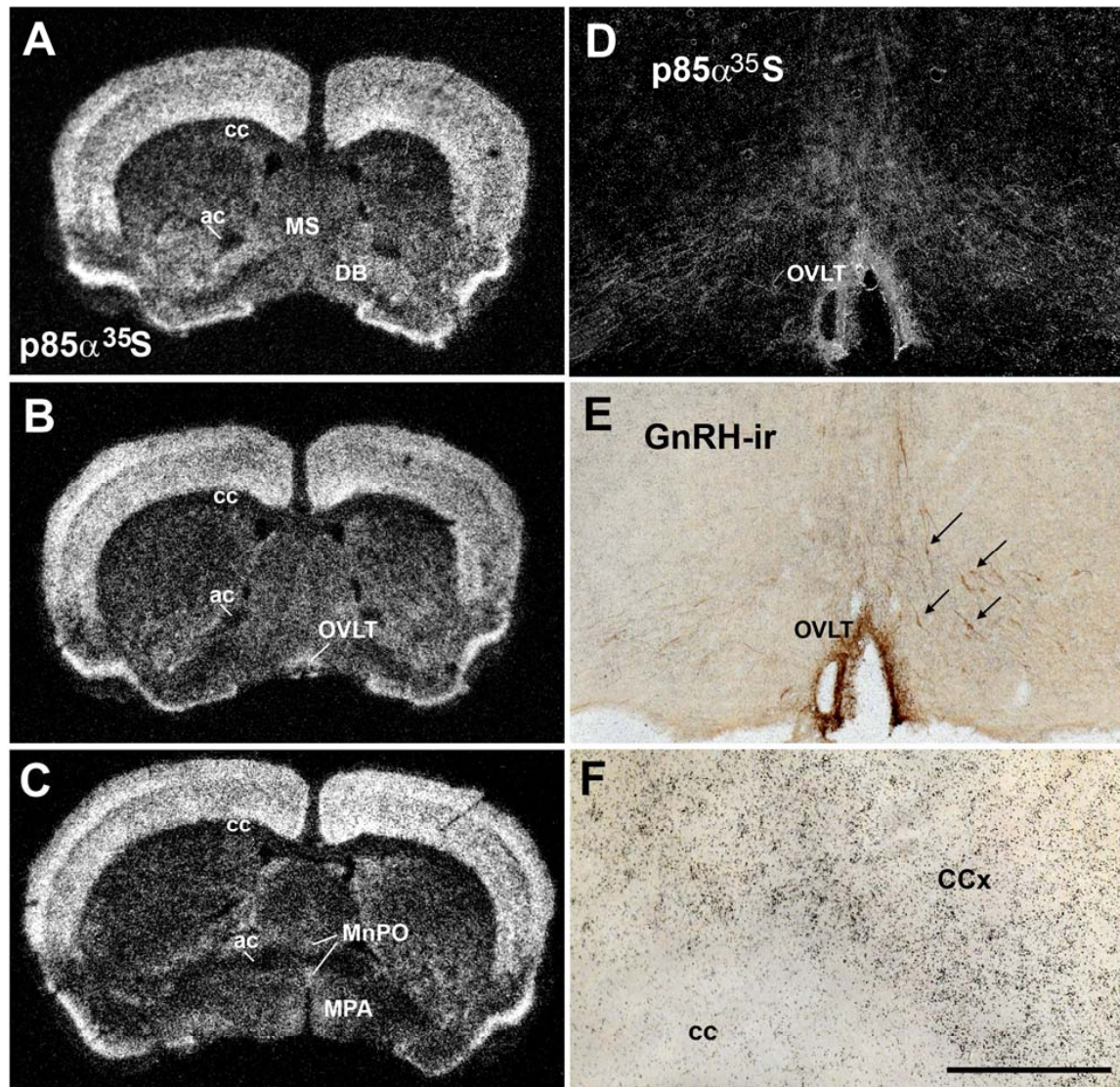
**Supplemental Fig. 1:** Breeding scheme for the generation of GnRH-p85αKO mice.



**Intercross:**



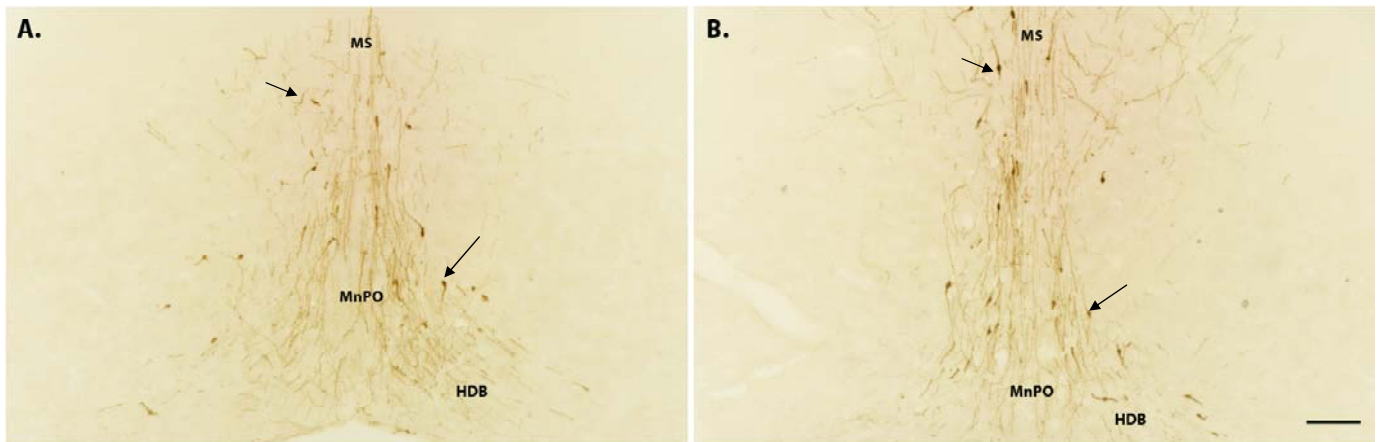
**Supplemental Fig. 2:** Breeding scheme for the generation of GnRH-p85DKO mice. After generating p85<sup>flx/flx</sup>/β<sup>-/+</sup> animals (homozygous for “floxed” *Pik3r1* and heterozygous for *Pik3r2* KO, highlighted in bold above), a male or a female that was also GnRH-CRE<sup>+</sup> was crossed with a GnRH-CRE<sup>-</sup> animal.



**Supplemental Fig. 3:** The phosphatidylinositol-3 kinase subunit  $p85\alpha$  is abundantly expressed in the mouse brain. Coronal brain sections were hybridized with a  $^{35}\text{S}$ -labeled unique probe for  $p85\alpha$ . High expression is observed in areas containing GnRH neurons such as the medial septal nucleus (A; MS), organum vasculosum of the lamina terminalis (B; OVLT) and medial preoptic area (C; MPA). D and E depict darkfield and brightfield micrographs of the same sections, respectively. Arrows in E point to GnRH immunoreactive neurons in brown (GnRH-ir). F: brightfield micrographs to illustrate high hybridization signal in the cortex (CCx) vs. background signal in the corpus callosum (cc). ac, anterior commissure; DB, diagonal band area; MnPO, median preoptic nucleus. Scale bar = 250  $\mu\text{m}$ .



**Supplemental Fig. 4:** Representative brightlight micrographs showing background hybridization signal in the corpus callosum (A, cc) and in a GnRH neuron from a GnRH-p85 $\alpha$ KO mouse (B). C: a representative GnRH neuron from a WT animal showing p85 $\alpha$  mRNA levels above background. All three micrographs were taken at the same magnification using an ApoTome microscope. Images were acquired in black and white and later pseudo colored. Scale bar = 25  $\mu$ m

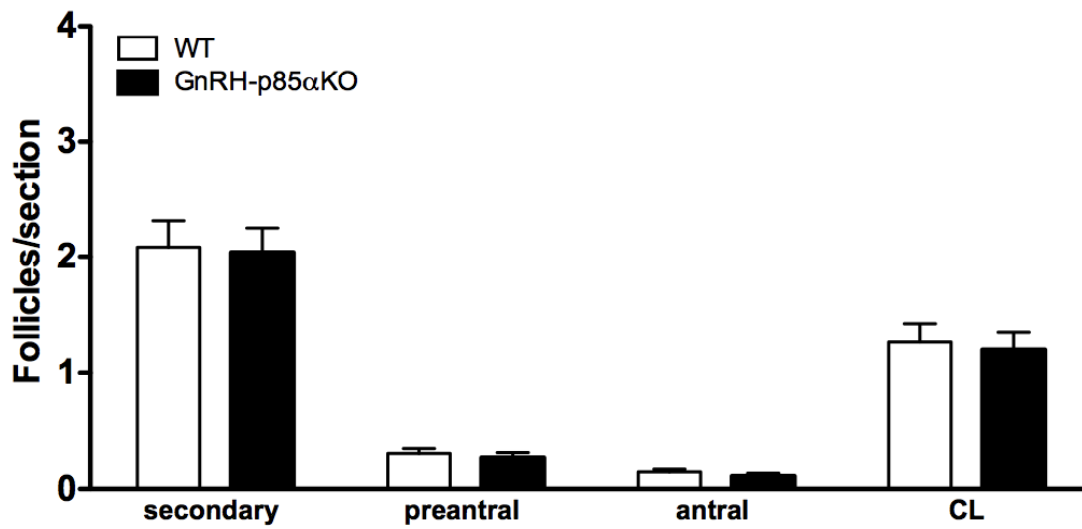


**Supplemental Fig. 5:** Representative brightlight micrographs showing GnRH immunoreactive neurons (brown staining pointed by arrows) in brain sections from WT (A) and GnRH-p85 $\alpha$ KO (B) animals. MS, medial septum; MnPO, median preoptic nucleus; HDB, horizontal diagonal band of Broca. Scale bar = 50  $\mu$ m.

### ***Histological analyses of ovaries and testes***

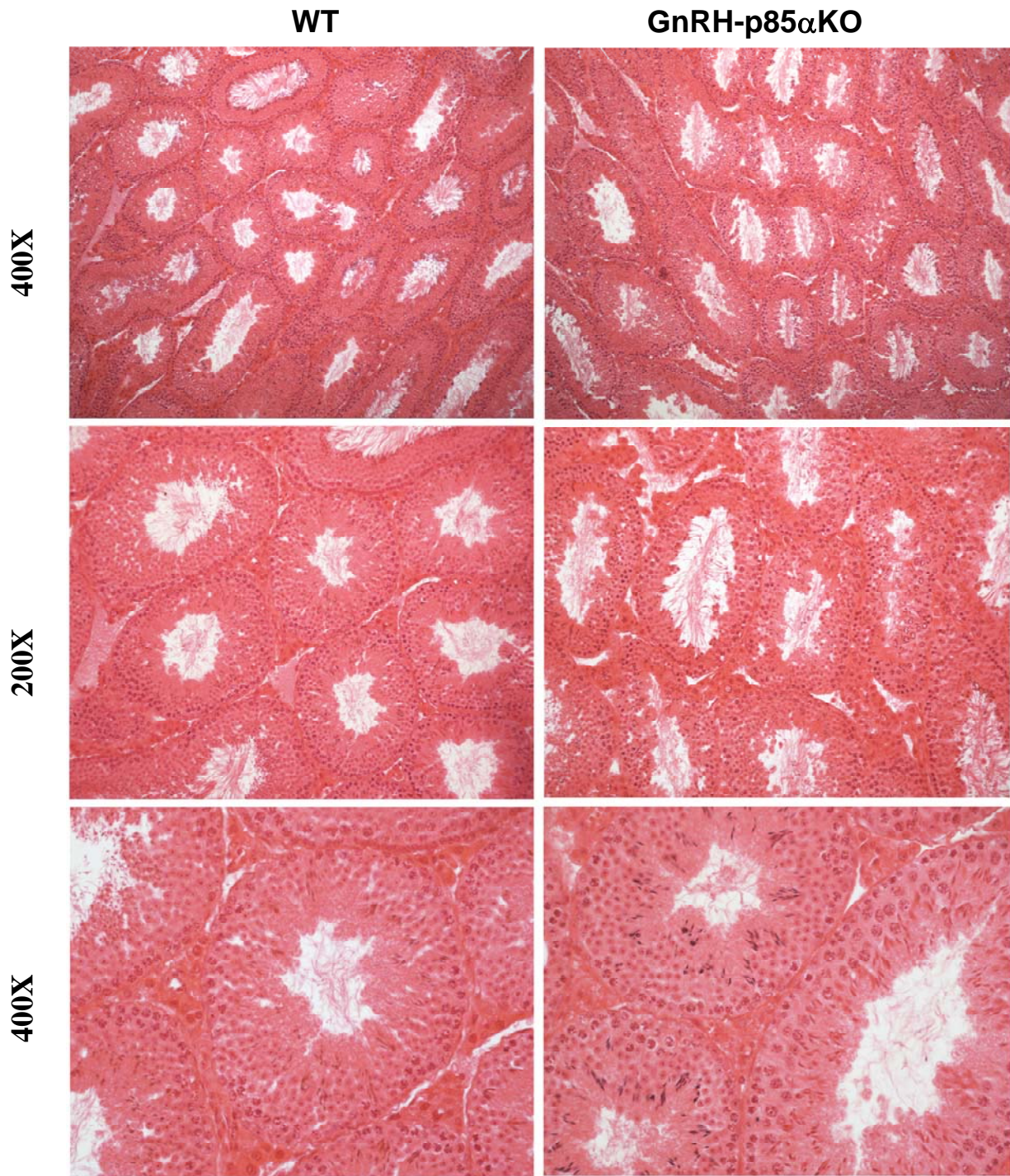
Ovaries were taken from adult (4-6 months) mice, fixed in 4% paraformaldehyde, paraffin embedded, sectioned and stained with hematoxylin and eosin. One ovary per animal was used for follicle counts. Follicles were counted every 10<sup>th</sup> section, beginning with the 5<sup>th</sup> section, through the entire ovary in a blinded fashion. Only follicles with a visible nucleus were counted. In addition, follicles were categorized as *secondary*, *preantral* or *antral*. Follicles were categorized as *secondary* if they contained an oocyte surrounded by two or more layers of granulose cells. *Preantral* follicles were identified if they had a central oocyte surrounded by layered granulose cells and containing fluid-filled areas within the granulose cell layer. Follicles were categorized as *antral*, if they had a single cavity containing follicle fluid surrounded by a granulose cell layer of even thickness and a cumulus-cell enclosed oocyte. Total number of corpora lutea (CL) per section was also recorded. For each ovary, total number of follicles (per follicle class) present in the scored sections was normalized to the total number of scored sections from that ovary to obtain a mean follicle count per section (1).

Testes were collected from adult mice and weighed. For histological analysis testes samples were fixed in Bouin's reagent at room temperature. Before used they were rinsed extensively in a series of graded ethanol solutions. Paraffin-embedded 5- $\mu$ m sections were then stained hematoxylin as previously described (2).



**Supplemental Fig. 6:** Follicle population in ovaries of adult WT and GnRH-p85αKO animals. Shown is the mean number of follicles per section for each follicle class per genotype ( $\pm$  SEM).



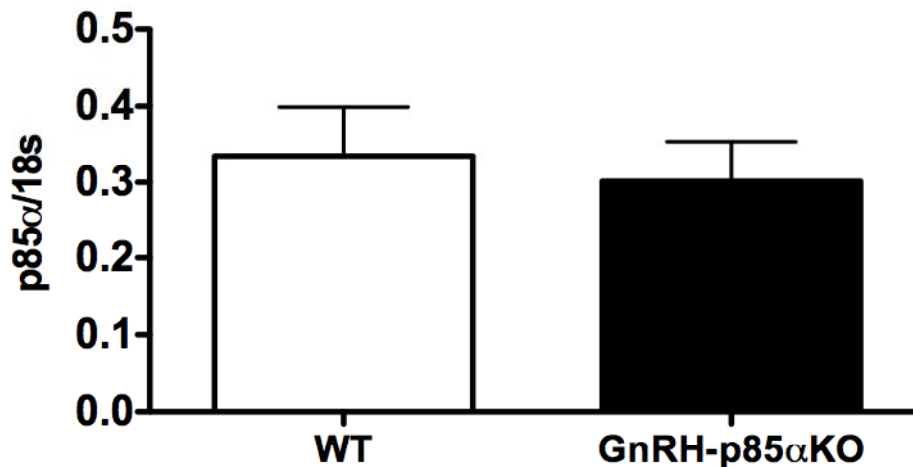


**Supplemental Fig. 7:** Representative photomicrographs of sections of testes from WT and GnRH-p85 $\alpha$ KO mice. No gross morphological effects were observed in the testicular tissue of mice carrying a GnRH-neuron-specific deletion of p85 $\alpha$  compared to WT animals.



### **RNA extraction, RT-PCR, and quantitative real-time PCR**

Total RNA was extracted from individual testes of WT and GnRH-p85 $\alpha$ KO mice and purified using Trizol (Invitrogen, Carlsbad, CA) according to the manufacturer's instructions. RT-PCR has been described previously (3). Briefly, approximately 5  $\mu$ g total RNA were subjected to reverse transcription using random hexamer primers (Ambion Inc., Austin, TX, USA) and Maloney murine leukemia virus reverse transcriptase (10 U/ $\mu$ l, Promega). The Taqman Real Time PCR method in a 96-well plate format was used. Universal Taqman master mix and optimized primer and probe sets were purchased from Applied Biosystems (Foster City, CA) and used according to the manufacturer's recommendations in a 20  $\mu$ l volume.



**Supplemental Fig. 8:** No significant difference in the mRNA levels for p85 $\alpha$  in the testis of GnRH-p85 $\alpha$ KO males compared to WT littermates were found by Real Time PCR. 18s acts as an internal control. The results are means  $\pm$  SEM, n=6.

### **References**

1. **Emmen JM, Couse JF, Elmore SA, Yates MM, Kissling GE, Korach KS** 2005 In vitro growth and ovulation of follicles from ovaries of estrogen receptor (ER){alpha} and ER{beta} null mice indicate a role for ER{beta} in follicular maturation. *Endocrinology* 146:2817-2826
2. **Turgut G, Abban G, Turgut S, Take G** 2003 Effect of overdose zinc on mouse testis and its relation with sperm count and motility. *Biol Trace Elem Res* 96:271-279
3. **Chen M, Hsu I, Wolfe A, Radovick S, Huang K, Yu S, Chang C, Messing EM, Yeh S** 2009 Defects of prostate development and reproductive system in the estrogen receptor-alpha null male mice. *Endocrinology* 150:251-259